APPLIED AND ENVIRONMENTAL MICROBIOLOGY, Jan. 2007, p. 499–507 Vol. 73, No. 2
0099-2240/07/$08.00+0 doi:10.1128/AEM.02084-06
Copyright © 2007, American Society for Microbiology. All Rights Reserved.

Transcriptional and Metabolic Responses of *Bacillus subtilis* to the Availability of Organic Acids: Transcription Regulation Is Important but Not Sufficient To Account for Metabolic Adaptation▽†

Oliver Schilling,[1] Oliver Frick,[2] Christina Herzberg,[1] Armin Ehrenreich,[1] Elmar Heinzle,[2] Christoph Wittmann,[2] and Jörg Stülke[1]*

Abteilung Allgemeine Mikrobiologie, Institut für Mikrobiologie und Genetik, Georg-August-Universität Göttingen, Grisebachstr. 8, D-37077 Göttingen, Germany,[1] and Technische Biochemie, Universität des Saarlandes, P.O. Box 151150, D-66123 Saarbrücken, Germany[2]

Received 4 September 2006/Accepted 12 November 2006

The soil bacterium *Bacillus subtilis* can use sugars or organic acids as sources of carbon and energy. These nutrients are metabolized by glycolysis, the pentose phosphate pathway, and the Krebs citric acid cycle. While the response of *B. subtilis* to the availability of sugars is well understood, much less is known about the changes in metabolism if organic acids feeding into the Krebs cycle are provided. If *B. subtilis* is supplied with succinate and glutamate in addition to glucose, the cells readjust their metabolism as determined by transcriptome and metabolic flux analyses. The portion of glucose-6-phosphate that feeds into the pentose phosphate pathway is significantly increased in the presence of organic acids. Similarly, important changes were detected at the level of pyruvate and acetyl coenzyme A (acetyl-CoA). In the presence of organic acids, oxaloacetate formation is strongly reduced, whereas the formation of lactate is significantly increased. The *alsSD* operon required for acetoin formation is strongly induced in the presence of organic acids; however, no acetoin formation was observed. The recently discovered phosphorylation of acetolactate decarboxylase may provide an additional level of control of metabolism. In the presence of organic acids, both types of analyses suggest that acetyl-CoA was catabolized to acetate rather than used for feeding the Krebs cycle. Our results suggest that future work has to concentrate on the posttranslational mechanisms of metabolic regulation.

Bacillus subtilis and its close relatives are among the most important industrial microorganisms. They are used for the production of antibiotics, enzymes such as proteases, amylases, lipases, or cellulases, vitamins such as riboflavin, and even insecticidal proteins. Due to this practical relevance, much research has been devoted to many aspects of these bacteria, making *B. subtilis* one of the best-studied living organisms.

The basis for understanding the potential of *B. subtilis* is a firm knowledge of its metabolism. These bacteria prefer sugars and ammonia as carbon and nitrogen sources, respectively. The preferred source of carbon and energy is glucose. This sugar is taken up and concomitantly phosphorylated by the bacterial phosphoenolpyruvate:sugar phosphotransferase system. The further metabolism involves glycolysis, the pentose phosphate pathway, and the Krebs cycle, resulting in the oxidation of glucose to carbon dioxide and the generation of ATP, a proton-motive force, reducing power, and intermediates for all anabolic reactions. Similarly, other sugars and polyols can be phosphorylated and are catabolized in a similar manner (for a review, see reference 35). The utilization of organic acids requires the conversion of these acids to intermediates of the Krebs cycle, gluconeogenesis, and the pentose phosphate pathway to obtain both the energy and the metabolic precursors needed by the cell (13). The central intermediate of nitrogen metabolism is glutamate, the universal amino-group donor for the biosynthesis of amino acids, nucleotides, and all other nitrogen-containing compounds in the cells (for a review, see reference 17).

The details of the central carbon and nitrogen metabolic pathways in *B. subtilis* and their regulation have been the subject of extensive investigations. The *ptsGHI* operon, encoding the general and glucose-specific phosphotransferase system proteins, is induced by glucose due to a mechanism of transcriptional antitermination (30, 34). The glycolytic enzymes that are needed for reversible reactions are constitutively transcribed, whereas those that catalyze irreversible reactions (*pfkA*, *gapA*, and *pyk*, encoding phosphofructokinase, glyceraldehyde-3-phosphate dehydrogenase, and pyruvate kinase, respectively) are induced in the presence of glucose (16, 24). The complex *gapA* operon, containing six genes encoding enzymes of triose phosphate interconversions, is repressed by the CggR repressor in the absence of glycolytic substrates, and the mRNA is in addition subject to posttranscriptional processing. Moreover, an internal promoter ensures that those enzymes catalyzing reversible reactions are present under both glycolytic and gluconeogenic conditions (12, 26). The *pdhABCD* operon, encoding pyruvate dehydrogenase, the link between glycolysis and the Krebs cycle, is also induced by glucose by an as-yet-unknown mechanism (5). Several genes encoding en-

* Corresponding author. Mailing address: Department of General Microbiology, Institute of Microbiology and Genetics, Georg-August University Göttingen, Grisebachstr. 8, D-37077 Göttingen, Germany. Phone: 49-551-393781. Fax: 49-551-393808. E-mail: jstuelk@gwdg.de.

† Supplemental material for this article may be found at http://aem.asm.org/.

▽ Published ahead of print on 22 November 2006.

TABLE 1. *B. subtilis* strains used in this study

Strain	Genotype	Source or reference[a]
168	*trpC2*	Laboratory collection
BSIP1114	*trpC2 amyE*::(*pta-lacZ cat*)	28
GP133	*trpC2 amyE*::(*fbaA-lacZ cat*)	24
GP205	*trpC2 amyE*::(*citB-lacZ cat*)	6
GP216	*trpC2 amyE*::(*pdhA-lacZ cat*)	pGP721 → 168
GP250	*trpC2 amyE*::(*nrgA-lacZ aphA3*)	11
GP268	*trpC2 amyE*::(*glnR-lacZ aphA3*)	pGP189 → 168
GP313	*trpC2 amyE*::(*cggR-lacZ cat*)	24
GP314	*trpC2 amyE*::(*pgi-lacZ cat*)	24
GP315	*trpC2 amyE*::(*pfkA-lacZ cat*)	24
GP317	*trpC2 amyE*::(*pgk-lacZ cat*)	24
GP342	*trpC2 amyE*::(*gltA-lacZ aphA3*)	38
QB5556	*trpC2 amyE*::(*rocD′-′lacZ cat)*	18
QB7041	trpC2 *amyE*::(ΔCA*ptsG-lacZ cat*)	34

[a] Arrows indicate construction by transformation.

TABLE 2. Specific rates of growth, substrate consumption, and product formation and yields of *B. subtilis* cultivated on CG and CGSE

Measurement	Result for cultivation on:	
	CG	CGSE
Specific growth rate μ (h^{-1})	0.64	0.81
Specific rate (mmol g^{-1} h^{-1}) for:		
Glucose	−9.1	−10.0
Succinate	0	−1.0
Glutamate	0	−4.2
Acetate	5.3	8.3
Lactate	0	2.5
Pyruvate	0.1	0.6
Yield coefficient (mol mol^{-1}) for:		
Acetate	0.58	0.83
Lactate	0	0.25
Pyruvate	0.02	0.06
2-Oxoglutarate	0.01	0.06
Cell dry mass (g $mmol^{-1}$)	0.07	0.08

zymes of the Krebs cycle, such as *citZ* and *citB*, coding for the major citrate synthase and aconitase, respectively, are subject to a synergistic repression by glucose and a preferred nitrogen source such as glutamine. This repression is mediated by the LysR-type repressor protein CcpC (6, 20). Even though it is important under all conditions, not much is known about the regulation of the pentose phosphate pathway. A recent transcriptome study suggested that the genes encoding the enzymes of this pathway are constitutively expressed (5).

The assimilation of ammonium is initiated by its uptake by diffusion and by the AmtB (also designated NrgA) ammonium transporter at high and low ammonium concentrations, respectively (11). In *B. subtilis*, ammonium is assimilated exclusively by the glutamine synthetase/glutamate synthase pathway. Briefly, glutamine is synthesized from glutamate and ammonium, and the glutamine is used as the amino-group donor for the production of two molecules of glutamate with 2-oxoglutarate as the acceptor (4). The gene encoding glutamine synthetase (*glnA*) is controlled by the availability of glutamine through the GlnR repressor (31). The *gltAB* operon encoding glutamate synthase is subject to a dual control by the carbon and nitrogen sources: in the absence of ammonium, expression of the operon is repressed by the TnrA transcription factor, whereas transcription is activated by the GltC protein in the presence of sugars (3, 7, 38).

While much work has been devoted to the effects of the presence of glucose on gene expression and the cellular physiology of *B. subtilis*, relatively little is known about the response towards organic acids that feed into the Krebs cycle. These intermediates of the Krebs cycle and glutamate are known to induce specific transporters (1, 36, 44). Moreover, glutamate represses the genes of the Krebs cycle as long as ammonium and glucose are also available (6, 33). The impact of these Krebs cycle intermediates on the general metabolism has not been studied so far.

In this work, we investigated the response of *B. subtilis* to the presence of organic acids. This response was determined at the level of the subtranscriptome of genes of the central carbon and nitrogen metabolism and by assaying the carbon fluxes. Our results indicate that overflow metabolism, the Krebs cycle, and the reactions involved in the interconversions between glutamate and 2-oxoglutarate are strongly affected by the presence of the organic acids. Importantly, the data allow us to derive conclusions relating to possible posttranscriptional regulation events that had escaped attention until now.

MATERIALS AND METHODS

Bacterial strains, growth conditions, and enzyme assays. The *B. subtilis* strains used in this study are listed in Table 1. They are all isogenic derivatives of the strain 168. Bacteria were grown in C minimal medium supplemented with the auxotrophic requirement (tryptophan at 50 mg $liter^{-1}$) (15). Other media consisted of C medium supplemented with 99% [1-^{13}C]glucose (CG medium) or C medium supplemented with a mixture of 99% [1-^{13}C]glucose, succinate, and glutamate (CGSE medium). The labeled glucose was obtained from Campro Scientific (Veenendaal, The Netherlands). Glucose, succinate, and glutamate were added to final concentrations of 0.5%, 0.6%, and 0.8%, respectively (15). Parallel cultivations were performed in 500-ml shake flasks using a culture volume of 50 ml. The resulting physiological data on CG and CGSE are listed below (Table 2). Aliquots from identical cultures grown to mid-log phase (optical density at 600 nm of 1.5) were used for transcriptome and metabolic flux analyses. Quantitative assays of *lacZ* expression in *B. subtilis* were performed with cell extracts using *o*-nitrophenyl-β-galactopyranoside as the substrate, as described previously (25).

Plasmid constructions. Translational fusions with the *lacZ* gene were constructed using the vector pAC5 (25), which carries the pC194 chloramphenicol resistance gene *cat*, or the vector pAC7 (39), containing the kanamycin resistance gene *aphA3*. Both plasmids harbor a *lacZ* gene without a promoter located between two fragments of the *B. subtilis amyE* gene. Plasmid pGP189, containing a *glnR-lacZ* fusion, was constructed as follows. A 331-bp fragment containing the promoter region of the *glnRA* operon was amplified by PCR using the primers CD43 (5′AAAGAATTCCATTATGGCAGCAGGGACGTT) and CD44 (5′TC CTATTGGATCCAAAGGCATTGAGCG). The PCR products were digested with EcoRI and BamHI (restriction sites were introduced by PCR and are underlined in the primer sequences) and ligated with pAC7 linearized with the same enzymes. Similarly, plasmid pGP721, used for the construction of the *pdhA-lacZ* fusion, was obtained using the primers HMB49 (5′ CG GAATTCG ATGCTGCAGGCTATCGTG) and HMB50 (5′ CGGGATCCGCTTTTTTCG TTTTTGCAGCC) with pAC5 as the cloning vector.

RNA isolation and quality assessment. To isolate high-quality RNA suited for the detection of long transcripts and their precursors, the following procedure was used. The cells were harvested at the exponential phase. For RNA preparation, 12 ml of a cell suspension (optical density at 600 nm of 1.5) was used. After mechanical cell disruption, the frozen powder was instantly resuspended in 3 ml lysis buffer (4 M guanidine isothiocyanate, 0.025 M sodium acetate, pH 5.3,

TABLE 3. Calculated and experimentally detected ^{13}C labeling patterns of amino acids in cell hydrolysates of *B. subtilis* cultivated on CG and CGSE

Measured metabolite[a]	Result for cultivation on:					
	CG			CGSE		
	M_0	M_1	M_2	M_0	M_1	M_2
Alanine (*m/z* 260, C_{1-3})						
calc.	0.463	0.394	0.110	0.516	0.355	0.100
exp.	0.462	0.398	0.110	0.517	0.357	0.098
Valine (*m/z* 288, C_{1-5})						
calc.	0.280	0.416	0.212	0.345	0.404	0.183
exp.	0.279	0.419	0.212	0.344	0.405	0.183
Threonine (*m/z* 404, C_{1-4})						
calc.	0.305	0.388	0.206	0.560	0.273	0.123
exp.	0.305	0.385	0.206	0.560	0.273	0.122
Aspartate (*m/z* 418, C_{1-4})						
calc.	0.305	0.388	0.206	0.559	0.273	0.124
exp.	0.303	0.391	0.205	0.556	0.275	0.124
Glutamate (*m/z* 432, C_{1-5})						
calc.	0.205	0.365	0.264	0.629	0.231	0.107
exp.	0.204	0.364	0.264	0.629	0.231	0.107
Lysine (*m/z* 431, C_{1-6})						
calc.	0.192	0.357	0.271	0.376	0.366	0.173
exp.	0.198	0.352	0.267	0.374	0.367	0.174
Phenylalanine (*m/z* 336, C_{1-9})						
calc.	0.2396	0.3946	0.2476	0.2478	0.3847	0.2449
exp.	0.2389	0.3942	0.2477	0.2424	0.3943	0.2433
Tyrosine (*m/z* 466, C_{1-9})						
calc.	0.2063	0.3641	0.2616	0.2134	0.3564	0.2586
exp.	0.2071	0.3645	0.2621	0.2123	0.3630	0.2558

[a] calc., calculated values predicted by the solution of the mathematical model corresponding to the optimized set of fluxes; exp., experimental values obtained by gas chromatography-mass spectrometry analysis of *t*-butyl-dimethylsilyl-derivatized amino acids.

0.5% [wt/vol] *N*-laurylsarcosine). Subsequently, total RNA extraction with acid phenol solution was performed as described previously (24). The quality of the isolated RNA was tested by PCR to exclude the presence of traces of DNA and by Northern blot analysis to detect a large nonabundant mRNA (7.4 kb mRNA of the *gapA* operon) (24). Digoxigenin RNA probes specific for *gapA* (37) were used to detect the transcript of the *gapA* operon. The sizes of the RNA molecular weight markers (GIBCO BRL) were as follows: 9.49, 7.46, 4.40, 2.37, 1.35, and 0.24 kb.

Transcriptome analysis. The microarray slides contained 93 different PCR products of 300 to 500 bp in length, representing 70 genes of the central carbon and nitrogen metabolic pathways of *B. subtilis*. The PCR products correspond to the 3′ end of each gene. Additionally, selected genes were also present on the slides with 300 to 500 bp of the 5′ ends as a quality control. To avoid PCR artifacts due to unspecific priming, all PCR products were checked on an agarose gel and sequenced. The PCR products were purified using a QIAquick 96 PCR purification kit (QIAGEN, Hilden, Germany) on a BioRobot 8000 (QIAGEN, Hilden, Germany). The slides were produced by spotting the PCR products using a Lucidea (Amersham Biosciences, Freiburg, Germany) contact printer. Each gene was present with eight spots organized in two rows with four spots on the microarray slide. Each row originated from an independent PCR. For laser calibration, a custom-made scorecard, consisting of 10 PCR products of *Escherichia coli* and *Mycoplasma pneumoniae* genes (400 to 500 bp each), was used. These DNA fragments were spotted, and the absence of cross-hybridization with any of the labeled *B. subtilis* cDNAs was verified. Each spot contained 30 pg of probe DNA and was generated by placing 100 pl of a 50% aqueous dimethyl sulfoxide solution on amino-silane-coated Type 7* slides (Amersham Biosciences, Freiburg, Germany). The probes were cross-linked onto the slides by UV illumination (50 mJ/cm^2) after the total evaporation of the spotting solution. The arrays were stored in the dark in a vacuum desiccator.

cDNA labeling. The isolated RNA was used to generate cDNAs labeled with fluorescent Cy-3 and Cy-5 dyes according to a direct labeling protocol (19) with the following modifications. Annealing was performed with 25 μg of total *B. subtilis* RNA, 40 mU of RNA Guard (Amersham Biosciences, Germany), in vitro transcribed RNA of the 10 *E. coli* and *M. pneumoniae* genes (ranging from 1.5 to 25 ng) with defined ratios for the Cy-3 and Cy-5 reaction mixes (1:10, 10:1, 1:5, 5:1, and 1:1), and 1 μl specific primer mix (including primers of the 10 scorecard genes). Each primer was present in the primer mix at a concentration of 5 pM. Primer annealing was performed in a thermocycler by asymptotic cooling from 70°C to 22°C within 30 min. Then, fivefold reaction buffer, 200 U Superscript III reverse transcriptase (Invitrogen GmbH, Karlsruhe, Germany), 2 μl dithiothreitol (0.1 M), 1 μl deoxynucleoside triphosphate mix (10 mM ATP, GTP, TTP, 3 mM CTP), and 1 μl Cy-3 or Cy-5 dyes (Amersham Biosciences, Germany) were added. Incubation was performed for 2 hours at 42°C. The labeled cDNA was purified with a CyScribe GFX purification kit (Amersham Biosciences, Germany). Finally, the amount of incorporated fluorescent nucleotides was determined by measuring the absorption of the purified labeled cDNA at 550 nm for Cy-3 and at 650 nm for Cy-5. In each hybridization, equal amounts of incorporated fluorescent dye, ranging from 80 to 150 pmol, were used.

Hybridization. For hybridization, the fluorescently labeled cDNA was denatured for 2 min at 95°C followed by the addition of 50 μl microarray hybridization buffer (CyScribe first-strand cDNA labeling kit; Amersham Biosciences, Germany) and 110 μl formamide. Hybridization was carried out at 42°C overnight using an automatic sample processor (Lucidea SlidePro hybridization chamber; Amersham Biosciences, Germany) (19).

Microarray analysis: data normalization and evaluation. The signal intensities from each spot on the array were collected using a GenePix 4000B scanner and GenPix Pro software version 4.0 from Axon Instruments (Union City, CA). During a prescan at lower resolution, approximate normalization using the known concentrations of the scorecard was performed. The scan for data acquisition was then done at a 10-μm/pixel resolution. The calculation of the expression ratios for all genes was performed using the GenPix Pro 4.0 software. Three mathematically different ratios were calculated: ratio of medians, ratio of means, and regression ratio. To ensure data quality, the following two criteria were applied: (i) the signal intensities of both fluorescent dyes of a spot corrected for its calculated background had to be greater than the standard deviation of the background of the corresponding fluorescent dye, and (ii) the deviation of the expression ratio calculated by the three different methods had to be within a 30% interval. To generate two biologically independent experiments, RNA was extracted from two independent cultures grown in CG or CGSE minimal medium. One pair of RNA samples was additionally subjected to a dye-flip experiment. As each open reading frame was spotted eight times on each microarray slide (see above), 24 expression values were generated for evaluation if each passed the

quality control criteria. From at least 12 of the 24 potential values for each open reading frame, the average value of the ratio of median was calculated, and the standard deviations are shown elsewhere (see the supplemental material).

Mass spectrometric ^{13}C labeling analysis. Mass isotopomer fractions of amino acids from the cell protein were determined by gas chromatography-mass spectrometry (21, 43). For this purpose, cells (about 1 mg dry cell mass) were harvested from the culture and washed twice with deionized water. The pellet was then incubated with 50 μl 6 M HCl for 24 h at 105°C, subsequently neutralized with 6 M NaOH, and cleared from insoluble matter by centrifugation (5 min; Ultrafree-MC filter units and 0.22-μm Durapore membrane; Millipore, Bedford, MA). The remaining clear solution was lyophilized. Analysis of the amino acids was performed after derivatization into the *t*-butyl-dimethylsilyl derivative (22, 40). All samples were first measured in scan mode to check for potential isobaric interference between analytes and other sample components. The labeling patterns of the amino acids were then determined in triplicate via selective ion monitoring of selected ion clusters, representing [M-57] fragments with the complete carbon skeletons of the amino acids. The mean experimental error for the mass isotopomer fractions was about 0.15%.

Metabolic modeling and parameter estimation. The metabolic network for growth of *B. subtilis* on CG or CGSE comprised all central metabolic pathways, i.e., glycolysis, the pentose phosphate pathway, the Krebs cycle, and anaplerotic carboxylation. Additionally, the pathways for the formation of lactic acid, acetic acid, acetoine, and glycerol and the anabolic pathways from intermediary precursors into biomass were implemented. For glycine synthesis, two possible routes, i.e., via serine and via threonine aldolase, were considered (32). Calculation of the anabolic demands for the different precursors was based on literature data on the biomass composition of *B. subtilis*, previously determined as a function of growth rate (9, 10). The exact demands for both studied conditions was interpolated from these literature data depending on the specific growth rate measured in the present work (Table 2).

Labeling data for proteinogenic amino acids and for glucose from all carbohydrates and the mean values of the stoichiometric data from two parallel cultivations were combined for a calculation of metabolic flux. The set of fluxes that gave minimum deviation between experimental ($M_{i,exp}$) and simulated ($M_{i,calc}$) mass isotopomer fractions was taken as the best estimate for the intracellular flux distribution. The network was overdetermined, so that a least-squares approach was possible. As the error criterion, a weighted sum of least squares was used (42). All metabolic simulations were carried out on a personal computer by use of Matlab 7.0 (Mathworks Inc., Natick, MA). Details on the computational tools are given elsewhere (41, 42, 43). For the flux distributions, an excellent agreement between experimentally detected and calculated labeling patterns was achieved. The deviation between measured and calculated mass isotopomers was typically below 3% and thus rather small (Table 3). Flux distributions, including deviations within intervals of 90% confidence, are shown in Fig. 1. The confidence intervals were calculated by a Monte Carlo approach as described previously (42).

RESULTS AND DISCUSSION

Regulation of glycolysis. The expression of glycolytic genes was assayed by microarray analysis. The promoter activities of several glycolytic genes and operons were additionally studied by measuring β-galactosidase activities driven by these promoters. The transcriptome data suggested that the expression of glycolytic enzymes was only marginally affected by the addition of succinate and glutamate to the medium. These results are well supported by the comparison of the expression of *lacZ* fusions to promoters of glycolytic genes (Table 4). As judged from these expression data, the *ptsGHI* and *gapA* operons are highly transcribed under both conditions studied here, whereas the other promoters (*pgi*, *pfkA*, *fbaA*, and *pgk*) exhibit an intermediate activity (between 50 and 100 units of β-galactosidase/mg of protein). These results are in good agreement with previous findings, which demonstrated induction of *ptsGHI*, *gapA*, and *pfkA-pyk* expression in the presence of glucose to levels similar to those observed in this study (5, 24).

The results of the transcription analysis demonstrate that the transcription of glycolytic genes and operons is unaffected by the presence of glutamate and succinate as long as glucose is present in the medium. This conclusion is supported and extended by the metabolic flux analysis: with the notable exception of the reaction catalyzed by phosphoglucoisomerase (Pgi), the flux of the carbon skeletons derived from glucose through glycolysis is not affected by the presence of the organic acids. Thus, the activity of the glycolytic enzymes remains constant in addition to their expression (with the exception of phosphoglucoisomerase [see below]).

The partition of glucose-6-phosphate and the pentose phosphate pathway. Starting with glucose as the external substrate, glucose-6-phosphate is the first intracellular metabolite that is used by more than one enzyme. In CG minimal medium, glucose-6-phosphate is used by the glycolytic enzyme phosphoglucoisomerase (Pgi), and about one-third is catabolized to ribulose-5-phosphate due to the activity of glucose-6-phosphate dehydrogenase (Zwf) and the further enzymes of the pentose phosphate pathway. Finally, a small amount (about 2.5%) is used for the synthesis of biomass such as the cell wall. In the presence of glutamate and succinate, significantly less glucose-6-phosphate is converted to fructose-6-phosphate by the phosphoglucoisomerase than in the absence of the organic acids (54.8% compared to 64.4% relative to the total amount of glucose) (Fig. 1). Similarly, relatively less glucose-6-phosphate is used for biosynthetic purposes under these conditions. This might result from the availability of glutamate and succinate as precursors for many amino acids that have to be produced from the glucose in CG but not in CGSE medium. In contrast, the portion of glucose-6-phosphate that is oxidized by glucose-6-phosphate dehydrogenase is significantly increased (43.7% compared to 33.2%). This regulation of glucose-6-phosphate partition is not reflected by the transcriptional regulation of the genes encoding the two major enzymes that use glucose-6-phosphate as a substrate, i.e., *pgi* and *zwf*, which are constitutively expressed under the conditions used here. Previous studies indicated that the expression of these genes is also not affected by the presence of glucose in the medium (5, 24). A candidate that might cause the increased flux through the pentose phosphate pathway in the presence of succinate and glutamate is the *ywlF* gene, tentatively believed to encode ribulose-5-phosphate epimerase. The expression of this gene increased weakly but significantly upon the addition of the organic acids (Fig. 2). Moreover, both the transketolase (Tkt) and transaldolase (YwjH) were recently shown to be phosphorylated in vivo in *B. subtilis* (23). It is, however, unknown under which conditions these phosphorylations occur and how they affect the activities of the two enzymes. Due to the convergence of the pentose phosphate pathway with glycolysis at the fructose-6-phosphate and glyceraldehyde-3-phosphate levels, the changes in the partition of glucose-6-phosphate do not affect the fluxes through the lower part of glycolysis, which are essentially the same in both media (see above) (Fig. 1).

The partition of pyruvate and acetyl-CoA and the regulation of overflow metabolism. Pyruvate is among the most versatile metabolic intermediates. It can be oxidized to generate acetyl coenzyme A (acetyl-CoA) to enter the Krebs cycle (pyruvate dehydrogenase complex; *pdhABCD*), it can be converted to acetoin (acetolactate synthase and acetolactate decarboxylase; *alsS* and *alsD*, respectively), it can be reduced for the regeneration of NAD^+ (lactate dehydrogenase; *ldh*), and it can be

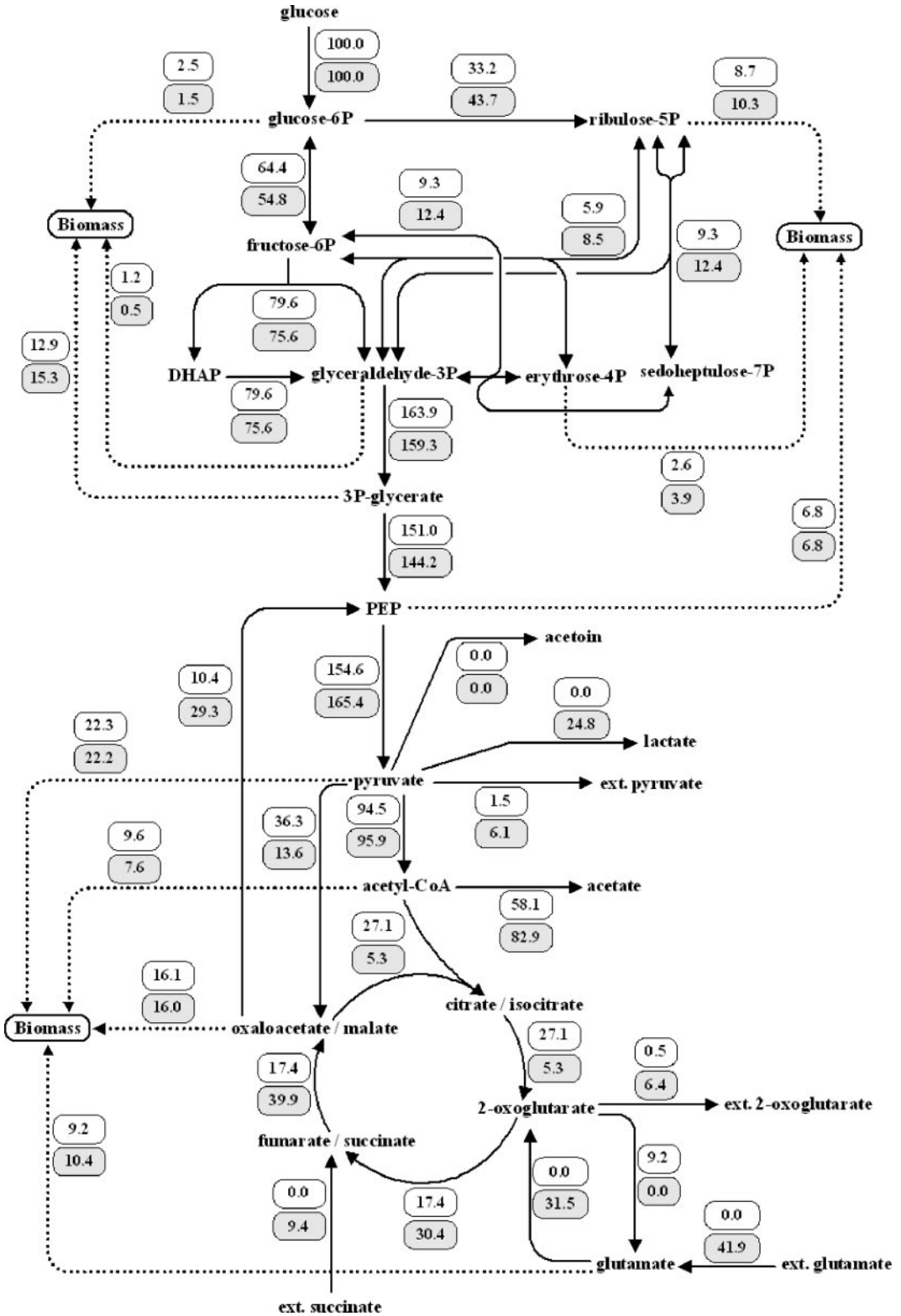

FIG. 1. Intracellular carbon flux distribution of *B. subtilis* cultivated on 99% [1-^{13}C]glucose under aerobic conditions in CG medium (white squares) and CSEG medium (gray squares). All fluxes are given as relative fluxes normalized to the specific glucose uptake rate (Table 2) including deviation values for 90% confidence. The fluxes correspond to the optimal fit between experimentally determined ^{13}C labeling patterns of amino acids of the cell protein and of glucose from cell carbohydrates and ^{13}C labeling patterns simulated via isotopomer modeling. PEP, phosphoenolpyruvate; DHAP, dihydroxyacetone phosphate; ext., external.

TABLE 4. Expression of genes of central metabolism in *B. subtilis* as judged from transcriptional fusions to the *lacZ* gene[a]

Strain	Gene/operon	β-Galactosidase activity with[b]:		CGSE/CG ratio by:	
		CG	CGSE	*lacZ* assay	Transcriptome analysis
QB7041	*ptsG*	603	649	1.07	0.99
GP314	*pgi*	56	53	0.94	1.06
GP315	*pfkA*	63	93	1.47	1.30
GP133	*fbaA*	95	83	0.88	1.20
GP313	*cggR* (*gapA*)	393	496	1.26	1.13
GP317	*pgk*	35	55	1.56	1.25
GP216	*pdhA*	110	145	1.32	1.69
BSIP1114	*pta*	50	220	4.30	1.67
GP205	*citB*	318	29	0.11	0.17
GP250	*nrgA*	2	1.8	0.90	0.98
GP268	*glnRA*	282	195	0.69	0.67
GP342	*gltA*	295	172	0.58	0.42
QB5556	*rocD*	12	12	1.00	1.17

[a] The regulation of the indicated genes was determined using the results of the reporter gene studies as well as those of the transcriptome analysis.

[b] Bacteria were grown in CG or CGSE minimal medium containing glucose. All strains contain transcriptional fusions of the promoter regions of the indicated genes to a promoterless *lacZ* gene. β-Galactosidase activities are given as units/mg of protein. Experiments were done in duplicate or triplicate. Representative results are shown.

used as an acceptor of carbon dioxide to replenish the Krebs cycle (pyruvate carboxylase; *pycA*). Moreover, the synthesis of several amino acids requires pyruvate as a precursor. Finally, pyruvate can be excreted into the medium.

The transcriptome data revealed that expression of the pyruvate dehydrogenase complex (*pdhABCD*) is weakly but significantly increased in the presence of the organic acids. This observation is supported by an assay of the β-galactosidase activity driven by the *pdhA* promoter (Table 4). However, this increase is not paralleled by an increased formation of acetyl-CoA from pyruvate in the presence of glutamate and succinate (probably due to the high activity of lactate dehydrogenase under these conditions [see below]).

Acetyl-CoA can be transferred to oxaloacetate to initiate the Krebs cycle (citrate synthase [CitZ]) for substrate level phosphorylation (generation of acetate involving phosphotransacetylase Pta and acetate kinase AckA [see below]) or for biosynthetic purposes. In the presence of glucose, *B. subtilis* is known to excrete large amounts of acetate. Indeed, significant acetate production was observed for CG medium. This acetate production was even strongly increased if glutamate and succinate were present (CGSE medium) (Fig. 1). This increased acetate excretion corresponds well with the increased transcription of the *pta* and *ackA* genes, encoding phosphotransacetylase and acetate kinase, respectively, as detected in the transcriptome analysis. Finally, the *pta* promoter was found to be stimulated fourfold by the presence of glutamate and succinate (Table 4). In contrast, the flux of acetyl-CoA into the tricarboxylic acid branch of the Krebs cycle was severely reduced in the presence of glutamate and succinate (Fig. 1). The reduction of citrate formation from acetyl-CoA is probably due to the fivefold reduced expression of *citZ*, encoding the major citrate synthase of *B. subtilis* in CGSE medium. Since the citrate synthase works according to the Michaelis-Menten kinetics, the fivefold repression in *citZ* expression results in a fivefold reduced flux of acetyl-CoA into the Krebs cycle. This may reflect the lack of need of the Krebs cycle if glucose, as a source of carbon and energy, and glutamate and succinate, as Krebs cycle intermediates, are available for the cell.

As long as glucose is present in excess, *B. subtilis* produces acetate to benefit from the additional substrate-level phosphorylation. However, the accumulation of acetate results in (i) the acidification of the medium (37) and (ii) the induction of the *alsSD* operon, encoding acetolactate synthase and acetolactate decarboxylase, and the subsequent synthesis of acetoin (8). It is not known whether the decrease of the pH or the accumulation of acetate triggers AlsR, the transcription activator of the *alsSD* operon. Our microarray study revealed that transcription of the *alsSD* operon is strongly induced by the presence of glutamate and succinate (10-fold induction of *alsS*) (Fig. 2). In this experiment, the pH value of the culture medium decreased from 7.17 to 7.01 on CG and from 7.33 to 7.04 on CGSE. The nearly constant pH of the culture medium suggests that the accumulation of acetate is the primary trigger of AlsR activity. However, no excretion of acetoin was observed under either condition. This may be due to the fact that acetoin might have just started to accumulate and thus been below the detection limit even if the genes were actively transcribed. Alternatively, the translation or the activity of acetolactate synthase and/or acetolactate decarboxylase might be controlled at an additional level. Indeed, the phosphorylation of acetolactate decarboxylase was recently reported (23). The expression of the *ldh* gene encoding lactate dehydrogenase is induced more weakly in CGSE medium than in CG medium. However, no excretion of lactate was detected in CG medium, whereas significant amounts of lactate were detected in the medium of the culture grown in the presence of glutamate and succinate.

If glucose is provided as the only carbon source (as in CG medium), the growth of *B. subtilis* depends on the activity of pyruvate carboxylase to replenish the Krebs cycle. Indeed, a significant portion of pyruvate is used for oxaloacetate production. In the presence of glutamate and succinate, the anaplerotic reactions are less important. This idea is supported by the finding that the flux of pyruvate to oxaloacetate is reduced about threefold in CGSE medium. This reduced flux is paralleled by a reduced expression of the *pycA* gene, which encodes pyruvate carboxylase, in CGSE medium relative to what is seen for CG medium. However, the regulation of *pycA* expression is much weaker than that of the flux through the reaction catalyzed by the pyruvate carboxylase. Thus, additional factors that control the activity of the enzyme may be involved. In both media, an important portion of pyruvate (about 12 to 15% of the total pyruvate pool) is used for the production of biomass. Finally, a small amount of pyruvate is excreted into the medium. Excretion is increased fourfold in CGSE medium; however, the proteins and gene products involved in pyruvate excretion have not yet been identified.

Regulation of the Krebs cycle. The Krebs cycle is central to the physiology of most heterotrophic organisms because it generates reducing power for respiration, precursors for anabolism, and an additional ATP in substrate-level phosphorylation. In *B. subtilis*, the expression of the genes encoding the initial enzymes of the Krebs cycle, citrate synthase and aconitase (*citZ* and *citB*, respectively), is synergistically repressed by glucose and glutamate/ammonium (6, 20). Our transcriptome

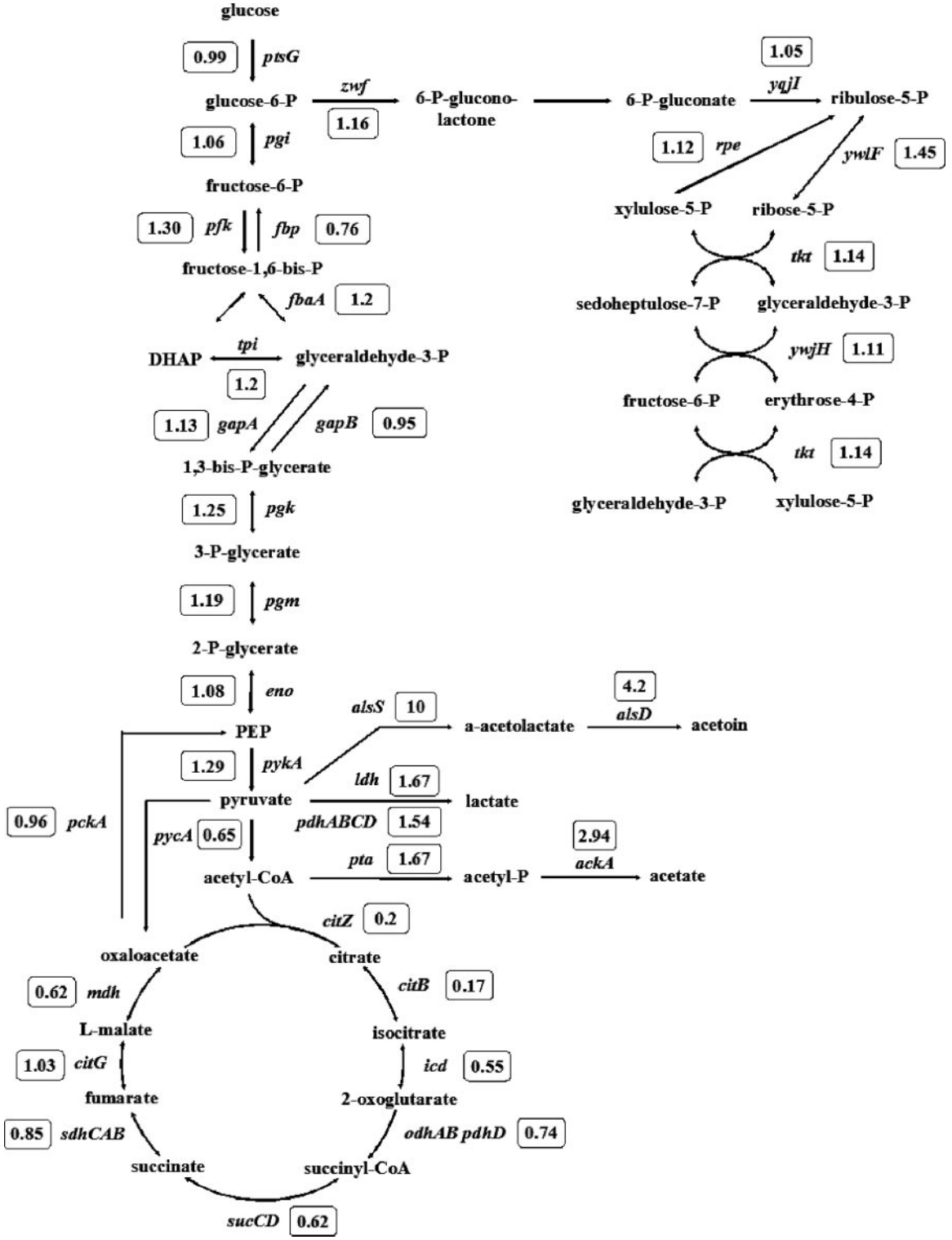

FIG. 2. Overview on the regulation of genes encoding enzymes of glycolysis, the pentose phosphate shunt, and the Krebs cycle in *B. subtilis*. The result of the transcriptome analysis is given next to each gene. The numbers correspond to the ratios of gene expression under the two conditions (CGSE/CG). For multisubunit enzymes encoded by operons, the mean factors of regulation of the genes of the operon are shown. A complete list of all studied genes is given elsewhere (see the supplemental material). PEP, phosphoenolpyruvate; DHAP, dihydroxyacetone phosphate.

analysis confirmed this regulatory pattern: both genes were repressed fivefold in CGSE medium (Fig. 2). Moreover, the activity of the *citB* promoter was repressed about tenfold by the presence of the organic acids in addition to glucose (Table 4). This repression of initial enzymes of the Krebs cycle is paralleled by the 4.6-fold reduction of carbon flow from acetyl-CoA to 2-oxoglutarate in CGSE from the level seen for CG medium. In the presence of externally provided glutamate and succinate, these acids can be taken up and glutamate can be converted to 2-oxoglutarate. As a result, the flux from glutamate to oxaloacetate was higher in CGSE than in CG medium. The genes of the enzymes catalyzing the reactions from 2-oxoglutarate to oxaloacetate were weakly regulated by the presence of organic acids. This reflects the need for these enzymes under both conditions studied in this work.

The genes encoding the transporters for succinate and glutamate, *dctP*, *gltP*, and *gltT*, are only weakly affected by the presence of organic acids. It should be noted, however, that *dctP* and *gltP* are subject to a catabolite repression in the presence of glucose (reference 5 and our unpublished results), suggesting that the two major transporters for succinate and glutamate are relatively weakly expressed under both conditions addressed in this study. In any case, significant amounts of glutamate and succinate were transported into the cells if these acids were available.

Regulation of nitrogen assimilation. The basic C medium used in this study contained ammonium, which can be transported into the cell by the NrgA (AmtB) transport protein and assimilated by the glutamine synthetase/glutamate synthase cycle made up of glutamine synthetase and glutamate synthase. In the presence of glutamate, neither the ammonium transporter nor the glutamate synthase is required for growth. The determination of the *nrgA* promoter activity demonstrated that the gene was not expressed in the two media studied here (Table 4). This is due to lack of transcription activation at high ammonium concentrations, which allow the entry of ammonia by diffusion (11). Similarly, the transcriptome data revealed that *nrgA* expression was not affected by the presence of glutamate. The expression of *glnA* was slightly repressed in CGSE medium. This may result from the reduced need for glutamine synthesis if glutamate is present in the medium: under these conditions, glutamine synthesis is required only to meet the need for this amino acid, while it is an intermediate in glutamate biosynthesis in CG medium. The *gltAB* operon, encoding the two subunits of glutamate synthase, was repressed about twofold by the addition of glutamate and succinate, as judged from both transcriptome and promoter fusion data (Table 4). Accordingly, no conversion of 2-oxoglutarate to glutamate was detectable in CGSE medium. The imported glutamate was used for biomass production (about 25% of the glutamate), and the remaining 75% was converted to 2-oxoglutarate by the action of glutamate dehydrogenase encoded by *rocG*. Interestingly, *rocG* expression was somewhat lower in the presence of glutamate and succinate. However, it should be mentioned that only basal *rocG* expression occurs in both CG and CGSE media, since the expression of *rocG* requires induction by arginine and moreover is repressed by glucose (2). Obviously, this low expression of glutamate dehydrogenase is sufficient to make a substantial contribution to feed the Krebs cycle in CGSE-grown bacteria. Thus, even though only weakly regulated at the level of transcription, the activities of the two enzymes interconverting 2-oxoglutarate and glutamate are mutually absolutely exclusive.

Conclusion. The metabolism of *B. subtilis* has evolved to adapt to a broad range of conditions of nutrient supply. This adaptation often involves changes in the transcription of the relevant genes. However, the *ldh* gene, encoding lactate dehydrogenase, is constitutively transcribed under the conditions studied here, even though lactate formation in CGSE medium is strongly increased compared to that in CG medium. In this case, the enzymatic activity of lactate dehydrogenase might be controlled, perhaps by the intracellular redox state. This suggestion is in good agreement with the observation that the expression of the *ldh* gene is controlled by the redox state of the cell in the presence of nitrate (29). On the other hand, some transcriptional regulation events are not paralleled by changes in the carbon fluxes. This was observed for the *alsSD* operon, required for acetoin biosynthesis. In this case, posttranslational control of AlsD activity by protein phosphorylation might account for an additional level of regulation. Phosphorylation is a common means to adjust protein activities to the metabolic requirements. However, only with the advance of proteomic methods can these modifications be detected (23). The role of protein phosphorylation in the control of metabolic pathways is well documented in the case of *E. coli* isocitrate dehydrogenase, and this phosphorylation also occurs in *B. subtilis* (14, 23). Moreover, the control of 2-oxoglutarate dehydrogenase activity by phosphorylation was recently discovered for *Corynebacterium glutamicum* (27). Thus, much work remains to be done to study the details of the regulatory events that occur at the different stages after transcription involving changes in mRNA stability, differential translation, and posttranslational modifications. This work will be essential for the development of systems biology.

ACKNOWLEDGMENTS

We are grateful to Irene Reif, Hans-Matti Blencke, and Christian Detsch for their help with the plasmid constructions. We thank Michel Fritz and Tae Hoon Yang for their assistance in analytics and valuable discussion.

This work was supported by grants from the Deutsche Forschungsgemeinschaft (Stu 214/4; He3092/6), the Federal Department of Education and Research, and the Fonds der Chemischen Industrie.

REFERENCES

1. **Asai, K., S. H. Baik, Y. Kasahara, S. Moriya, and N. Ogasawara.** 2000. Regulation of the transport system for C4-dicarboxylic acids in *Bacillus subtilis*. Microbiology **146:**263–271.
2. **Belitsky, B. R., and A. L. Sonenshein.** 1998. Role and regulation of *Bacillus subtilis* glutamate dehydrogenase genes. J. Bacteriol. **180:**6298–6305.
3. **Belitsky, B. R., L. V. Wray, Jr., S. H. Fisher, D. E. Bohannon, and A. L. Sonenshein.** 2000. Role of TnrA in nitrogen source-dependent repression of *Bacillus subtilis* glutamate synthase gene expression. J. Bacteriol. **182:**5939–5947.
4. **Belitsky, B. R.** 2002. Biosynthesis of amino acids of the glutamate and aspartate families, alanine, and polyamines, p. 203–231. *In* A. L. Sonenshein, J. A. Hoch, and R. Losick (ed.). *Bacillus subtilis* and its closest relatives: from genes to cells. ASM Press, Washington, DC.
5. **Blencke, H. M., G. Homuth, H. Ludwig, U. Mäder, M. Hecker, and J. Stülke.** 2003. Transcriptional profiling of gene expression in response to glucose in Bacillus subtilis: regulation of the central metabolic pathways. Metab. Eng. **5:**133–149.
6. **Blencke, H. M., I. Reif, F. M. Commichau, C. Detsch, I. Wacker, H. Ludwig, and J. Stülke.** 2006. Regulation of *citB* expression in *Bacillus subtilis*: integration of multiple metabolic signals in the citrate pool and by the general nitrogen regulatory system. Arch. Microbiol. **185:**136–146.
7. **Commichau, F. M., K. Forchhammer, and J. Stülke.** 2006. Regulatory links between carbon and nitrogen metabolism. Curr. Opin. Microbiol. **9:**167–172.

8. **Cruz Ramos, H., T. Hoffmann, M. Marino, H. Nedjari, E. Presecan-Siedel, O. Dreesen, P. Glaser, and D. Jahn.** 2000. Fermentative growth of *Bacillus subtilis*: physiology and regulation of gene expression. J. Bacteriol. **182:**3072–3080.
9. **Dauner, M., and U. Sauer.** 2001. Stoichiometric growth model for riboflavin-producing *Bacillus subtilis*. Biotechnol. Bioeng. **76:**132–143.
10. **Dauner, M., M. Sonderegger, M. Hochuli, T. Szyperski, K. Wüthrich, H. P. Hohmann, U. Sauer, and J. E. Bailey.** 2002. Intracellular carbon fluxes in riboflavin-producing *Bacillus subtilis* during growth on two-carbon substrate mixtures. Appl. Environ. Microbiol. **68:**1760–1771.
11. **Detsch, C., and J. Stülke.** 2003. Ammonium utilization in *Bacillus subtilis*: transport and regulatory functions of NrgA and NrgB. Microbiology **149:**3289–3297.
12. **Doan, T., and S. Aymerich.** 2003. Regulation of the central glycolytic pathways in *Bacillus subtilis*: binding of the repressor CggR to its single DNA target sequence is modulated by fructose-1,6-bisphosphate. Mol. Microbiol. **47:**1709–1721.
13. **Doan, T., P. Servant, S. Tojo, H. Yamaguchi, G. Lerondel, K. Yoshida, Y. Fujita, and S. Aymerich.** 2003. The *Bacillus subtilis ywkA* gene encodes a malic enzyme and its transcription is activated by the YufL/YufM two-component system in response to malate. Microbiology **149:**2331–2343.
14. **El-Mansi, M., A. J. Cozzone, J. Shiloach, and B. J. Eikmanns.** 2006. Control of carbon flux through enzymes of central and intermediary metabolism during growth of *Escherichia coli* on acetate. Curr. Opin. Microbiol. **9:**173–179.
15. **Faires, N., S. Tobisch, S. Bachem, I. Martin-Verstraete, M. Hecker, and J. Stülke.** 1999. The catabolite control protein CcpA controls ammonium assimilation in *Bacillus subtilis*. J. Mol. Microbiol. Biotechnol. **1:**141–148.
16. **Fillinger, S., S. Boschi-Muller, S. Azza, E. Dervyn, G. Branlant, and S. Aymerich.** 2000. Two glyceraldehyde-3-phosphate dehydrogenases with opposite physiological roles in a nonphotosynthetic bacterium. J. Biol. Chem. **275:**14031–14037.
17. **Fisher, S. H.** 1999. Regulation of nitrogen metabolism in *Bacillus subtilis*: vive la différence! Mol. Microbiol. **32:**223–232.
18. **Gardan, R., G. Rapoport, and M. Débarbouillé.** 1995. Expression of the *rocDEF* operon involved in arginine catabolism in *Bacillus subtilis*. J. Mol. Biol. **249:**843–856.
19. **Hovey, R., S. Lentes, A. Ehrenreich, K. Salmon, K. Saba, G. Gottschalk, R. P. Gunsalus, and U. Deppenmeier.** 2005. DNA microarray analysis of *Methanosarcina mazei* Gö1 reveals adaptation to different methanogenic substrates. Mol. Genet. Genomics **273:**225–239.
20. **Jourlin-Castelli, C., N. Mani, M. M. Nakano, and A. L. Sonenshein.** 2000. CcpC, a novel regulator of the LysR family required for glucose repression of the *citB* gene in *Bacillus subtilis*. J. Mol. Biol. **295:**865–878.
21. **Kiefer, P., E. Heinzle, O. Zelder, and C. Wittmann.** 2004. Comparative metabolic flux analysis of lysine-producing *Corynebacterium glutamicum* cultured on glucose or fructose. Appl. Environ. Microbiol. **70:**229–239.
22. **Krömer, J. O., O. Sorgenfrei, K. Klopprogge, E. Heinzle, and C. Wittmann.** 2004. In-depth profiling of lysine-producing *Corynebacterium glutamicum* by combined analysis of the transcriptome, metabolome, and fluxome. J. Bacteriol. **186:**1769–1784.
23. **Lévine, A., F. Vannier, C. Absalon, L. Kuhn, P. Jackson, E. Scrivener, V. Labas, J. Vinh, P. Courtney, J. Garin, and S. J. Séror.** 2006. Analysis of the dynamic Bacillus subtilis Ser/Thr/Tyr phosphoproteome implicated in a wide variety of cellular processes. Proteomics **6:**2157–2173.
24. **Ludwig, H., G. Homuth, M. Schmalisch, F. M. Dyka, M. Hecker, and J. Stülke.** 2001. Transcription of glycolytic genes and operons in *Bacillus subtilis*: evidence for the presence of multiple levels of control of the *gapA* operon. Mol. Microbiol. **41:**409–422.
25. **Martin-Verstraete, I. M. Débarbouillé, A. Klier, and G. Rapoport.** 1992. Mutagenesis of the *Bacillus subtilis* "-12, -24" promoter of the levanase operon and evidence for the existence of an upstream activating sequence. J. Mol. Biol. **226:**85–99.
26. **Meinken, C., H.-M. Blencke, H. Ludwig, and J. Stülke.** 2003. Expression of the glycolytic *gapA* operon in *Bacillus subtilis*: differential syntheses of proteins encoded by the operon. Microbiology **149:**751–761.
27. **Niebisch, A., A. Kabus, C. Schultz, B. Weil, and M. Bott.** 2006. Corynebacterial protein kinase G controls 2-oxoglutarate dehydrogenase activity via the phosphorylation status of the OdhI protein. J. Biol. Chem. **281:**12300–12307.
28. **Presecan-Siedel, E., A. Galinier, R. Longin, J. Deutscher, A. Danchin, P. Glaser, and I. Martin-Verstraete.** 1999. The catabolite regulation of the *pta* gene as part of carbon flow pathways in *Bacillus subtilis*. J. Bacteriol. **181:**6889–6897.
29. **Reents, H., R. Münch, T. Dammeyer, D. Jahn, and E. Härtig.** 2006. The Fnr regulon of *Bacillus subtilis*. J. Bacteriol. **188:**1103–1112.
30. **Schmalisch, M. H., S. Bachem, and J. Stülke.** 2003. Control of the *Bacillus subtilis* antiterminator protein GlcT by phosphorylation: elucidation of the phosphorylation chain leading to inactivation of GlcT. J. Biol. Chem. **278:**51108–51115.
31. **Schreier, H. J., S. W. Brown, K. D. Hirschi, J. F. Nomellini, and A. L. Sonenshein.** 1989. Regulation of *Bacillus subtilis* glutamine synthetase gene expression by the product of the *glnR* gene. J. Mol. Biol. **210:**51–63.
32. **Simic, P., J. Willuhn, H. Sahm, and L. Eggeling.** 2002. Identification of *glyA* (encoding serine hydroxymethyltransferase) and its use together with the exporter ThrE to increase L-threonine accumulation by *Corynebacterium glutamicum*. Appl. Environ. Microbiol. **68:**3321–3327.
33. **Sonenshein, A. L.** 2002 The Krebs citric acid cycle, p. 151–162. *In* A. L. Sonenshein, J. A. Hoch, and R. Losick (ed.). *Bacillus subtilis* and its closest relatives: from genes to cells. ASM Press, Washington, DC.
34. **Stülke, J., I. Martin-Verstraete, M. Zagorec, M. Rose, A. Klier, and G. Rapoport.** 1997. Induction of the *Bacillus subtilis ptsGHI* operon by glucose is controlled by a novel antiterminator, GlcT. Mol. Microbiol. **25:**65–78.
35. **Stülke, J., and W. Hillen.** 2000. Regulation of carbon catabolism in *Bacillus* species. Annu. Rev. Microbiol. **54:**849–880.
36. **Tanaka, K., K. Kobayashi, and N. Ogasawara.** 2003. The *Bacillus subtilis* YufLM two-component system regulates the expression of the malate transporters MaeN (YufR) and YflS, and is essential for utilization of malate in minimal medium. Microbiology **149:**2317–2329.
37. **Tobisch, S., D. Zühlke, J. Bernhardt, J. Stülke, and M. Hecker.** 1999. Role of CcpA in regulation of the central pathways of carbon catabolism in *Bacillus subtilis*. J. Bacteriol. **181:**6996–7004.
38. **Wacker, I., H. Ludwig, I. Reif, H. M. Blencke, C. Detsch, and J. Stülke.** 2003. The regulatory link between carbon and nitrogen metabolism in *Bacillus subtilis*: regulation of the *gltAB* operon by the catabolite control protein CcpA. Microbiology **149:**3001–3009.
39. **Weinrauch, Y., T. Msadek, F. Kunst, and D. Dubnau.** 1991. Sequence and properties of *comQ*, a new competence regulatory gene of *Bacillus subtilis*. J. Bacteriol. **173:**5685–5693.
40. **Wittmann, C., M. Hans, and E. Heinzle.** 2002. *In vivo* analysis of intracellular amino acid labelings by GC/MS. Anal. Biochem. **307:**379–382.
41. **Wittmann, C., and E. Heinzle.** 2001. Application of MALDI-TOF MS to lysine-producing *Corynebacterium glutamicum*: a novel approach for metabolic flux analysis. Eur. J. Biochem. **268:**2441–2455.
42. **Wittmann, C., and E. Heinzle.** 2002. Genealogy profiling through strain improvement by using metabolic network analysis: metabolic flux genealogy of several generations of lysine-producing corynebacteria. Appl. Environ. Microbiol. **68:**5843–5859.
43. **Wittmann, C., P. Kiefer, and O. Zelder.** 2004. Metabolic fluxes in *Corynebacterium glutamicum* during lysine production with sucrose as carbon source. Appl. Environ. Microbiol. **70:**7277–7287.
44. **Yamamoto, H., M. Murata, and J. Sekiguchi.** 2000. The CitST two-component system regulates the expression of the Mg-citrate transporter in *Bacillus subtilis*. Mol. Microbiol. **37:**898–912.